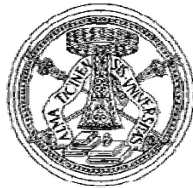


# Deep N-well CMOS MAPS with in-pixel signal processing and sparsification capabilities for the ILC vertex detector

G. Traversi, M. Manghisoni, L. Ratti, V. Re, V. Speciali



Università di Pavia  
*Dipartimento di Elettronica*



Università di Bergamo  
*Dipartimento di Ingegneria Industriale*



INFN  
*Sezione di Pavia*

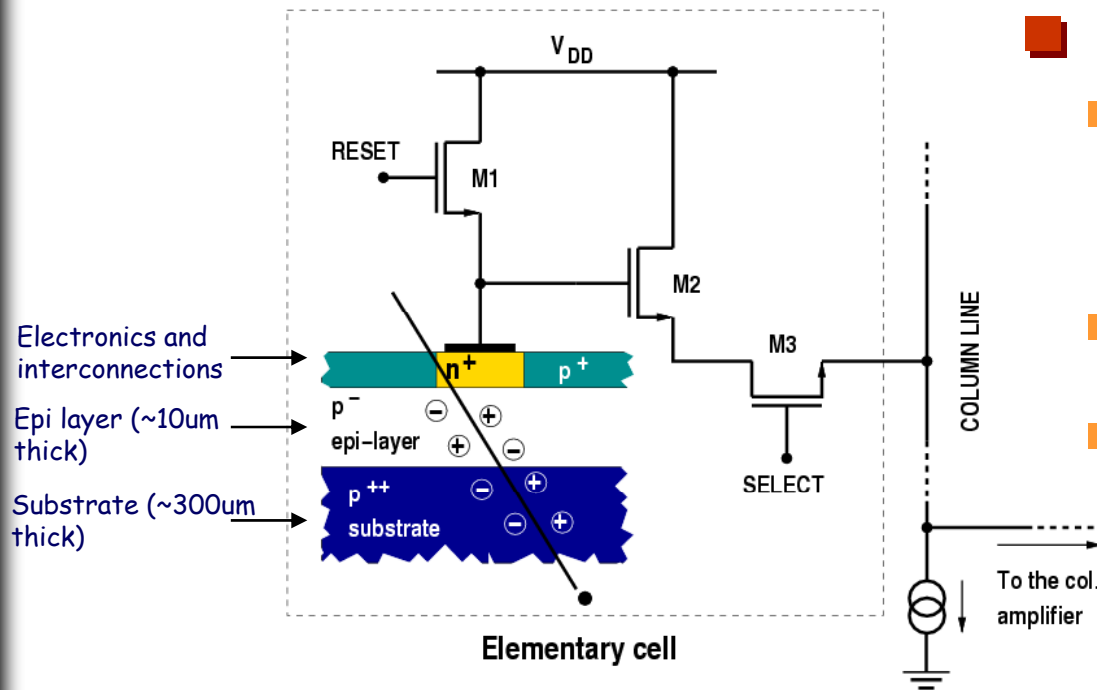
Vertex 2007 - 16<sup>th</sup> International Workshop on Vertex Detectors

September 23 - 28, 2007 - Lake Placid, NY, USA

# Outline

- Introduction: standard CMOS monolithic active pixel sensors
- Deep N-Well pixel sensor
- Description of the sensor level processor
- Digital section and digital readout scheme
- Physical simulations
- Conclusions

# Conventional CMOS MAPS



## Principle of operation:

- Signal generated by a particle is collected by an n-well/p-epitaxial diode, then readout by CMOS electronics integrated in the same substrate
- Charge generated by the incident particle moves by thermal diffusion
- Extremely simple in-pixel readout (3-T NMOS, PMOS not allowed)

## Several reasons make CMOS MAPS appealing as tracking devices:

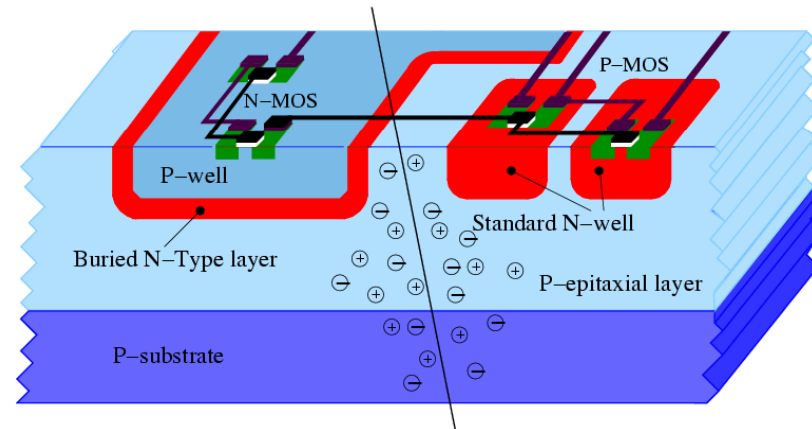
- Detector and readout on the same substrate
- Wafer can be thinned down to tens of  $\mu\text{m}$   $\Rightarrow$  minimal amount of material in the detector region (e.g. with respect to hybrid pixel)
- Deep sub-micron CMOS technology  $\Rightarrow$  high functional density and versatility, low power consumption, radiation tolerance and fabrication costs

# Deep Nwell sensor concept

- In triple-well CMOS processes a deep N-well is used to shield N-channel devices from substrate noise in mixed-signal circuits

- DNW MAPS is based on the same working principle as standard MAPS

- A DNW is used to collect the charge released in the epitaxial layer

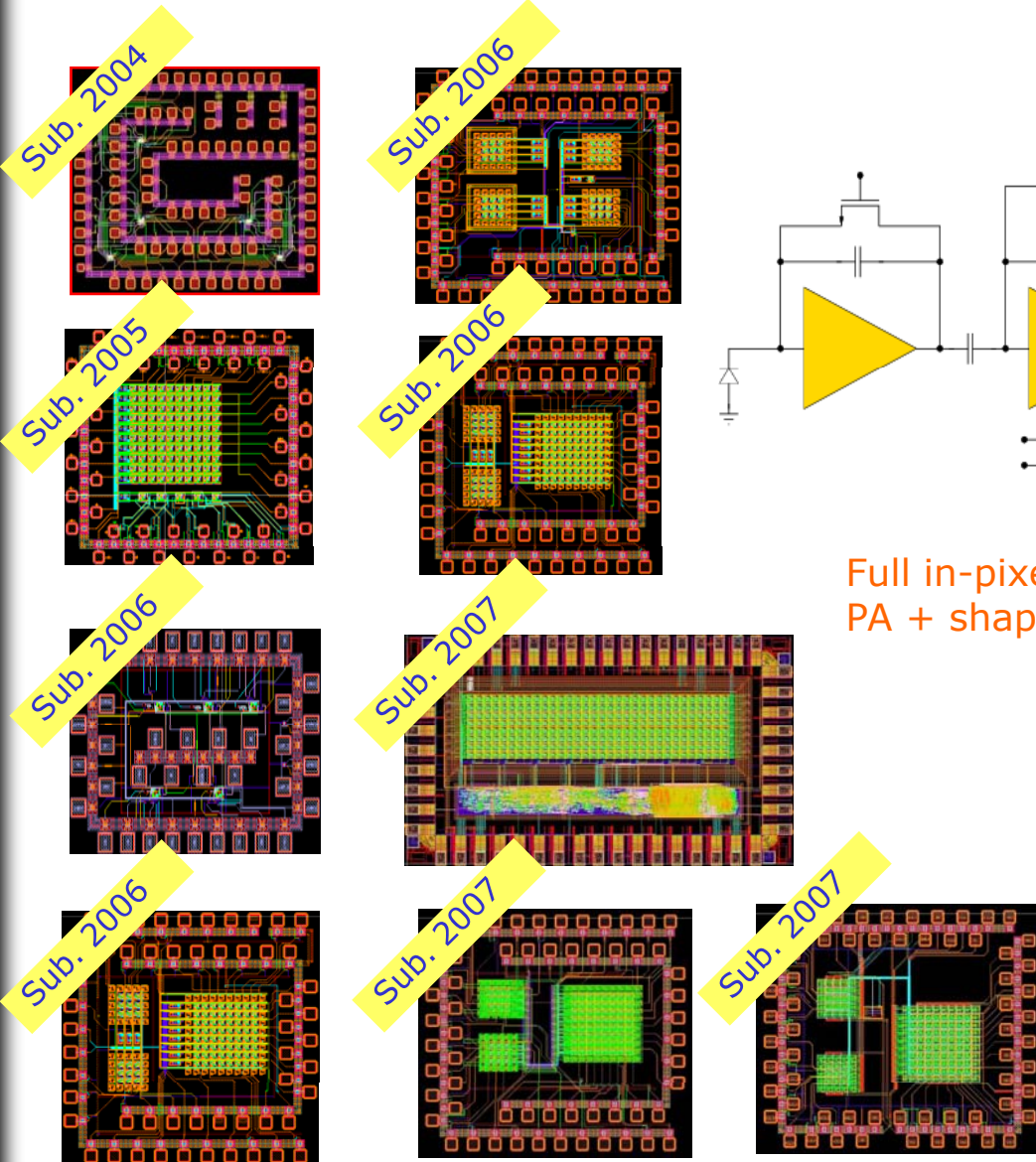


- A **charge preamplifier** is used for Q-V conversion → gain decoupled from electrode capacitance

- DNW may house **NMOS** transistors

- Using a large detector area, **PMOS devices** may be included in the front-end design → charge collection inefficiency depending on the ratio of the DNW area to the area of all the N-wells (deep and standard)

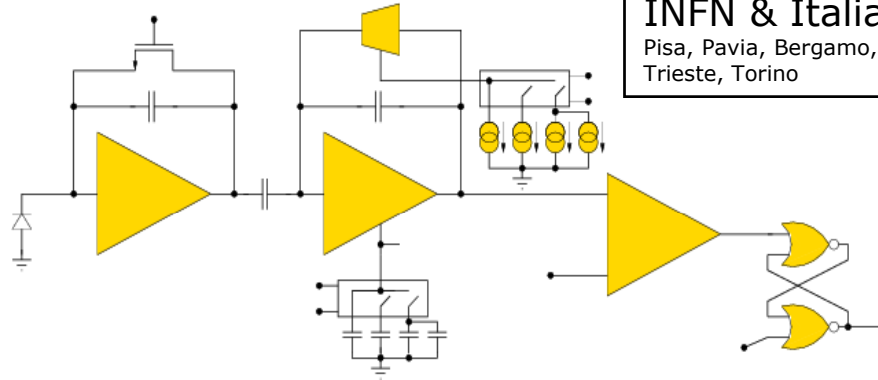
# APSEL series chips



SLIM5 Collaboration:

INFN & Italian Universities

Pisa, Pavia, Bergamo, Bologna, Trento,  
Trieste, Torino



Full in-pixel signal processing:  
PA + shaper + comparator + latch

Prototypes fabricated with the STMicroelectronics  
130nm triple-well technology

High sensitivity charge preamplifier with  
continuous reset + RC-CR shaper with  
programmable peaking time

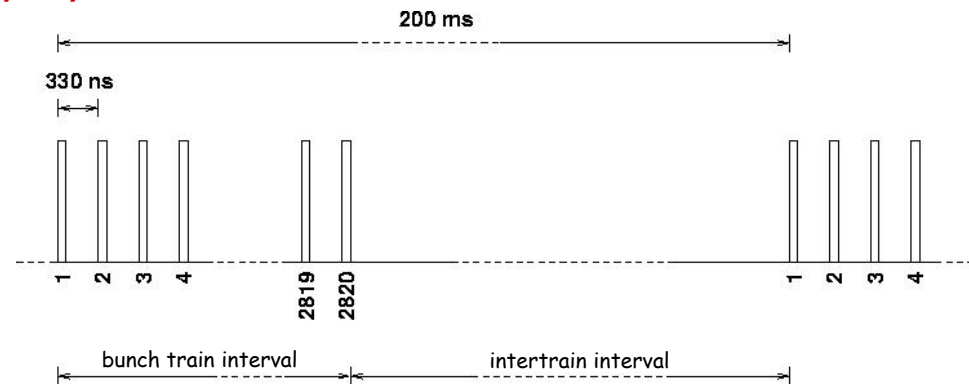
A threshold discriminator is used to drive a NOR  
latch featuring an external reset

Pixel size about  $50\mu\text{m} \times 50\mu\text{m}$

The first prototypes proved the capability of the  
sensor to collect charge from the epitaxial layer

# Design specifications for the ILC vertex detector

- The beam structure of ILC will feature 2820 crossings in a 1 ms bunch train, with a duty-cycle of 0.5%

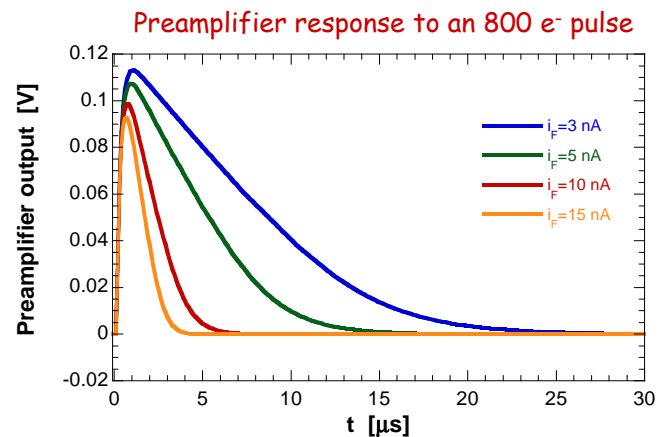
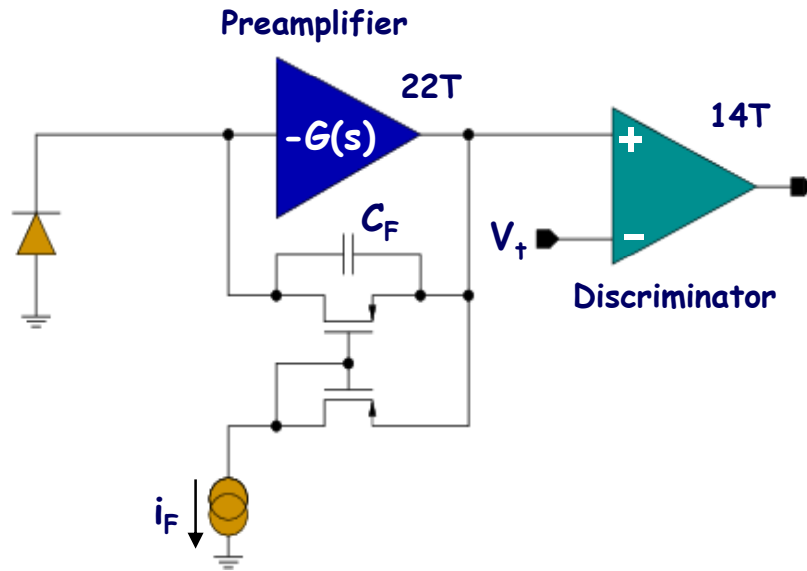


- assuming maximum hit occupancy  $0.03 \text{ part./Xing/mm}^2$
  - if 3 pixels fire for every particle hitting  $\rightarrow$  hit rate  $\approx 250 \text{ hits/train/mm}^2$
  - if a digital readout is adopted  $5 \mu\text{m}$  resolution requires  $17.3 \mu\text{m}$  pixel pitch
  - $15 \mu\text{m}$  pitch  $\rightarrow O_c \approx 0.056 \text{ hits/train} \rightarrow 0.0016$  probability of a pixel being hit at least twice in a bunch train period
- A pipeline with a depth of one in each cell should be sufficient to record  $> 99\%$  of events without ambiguity
  - Data can be readout in the intertrain interval  $\rightarrow$  system EMI insensitive

# Sparsified readout architecture

- In DNW MAPS sensors for ILC sparsification is based on a token passing readout scheme suggested by R. Yarema (R. Yarema, "Fermilab Initiatives in 3D Integrated Circuits and SOI Design for HEP", *ILC VTX Workshop at Ringberg, May 2006*)
  
- MAPS sensor operation is tailored on the structure of ILC beam
  - **Detection phase** (corresponding to the bunch train interval)
  - **Readout phase** (corresponding to the intertrain interval)

# Pixel level processor

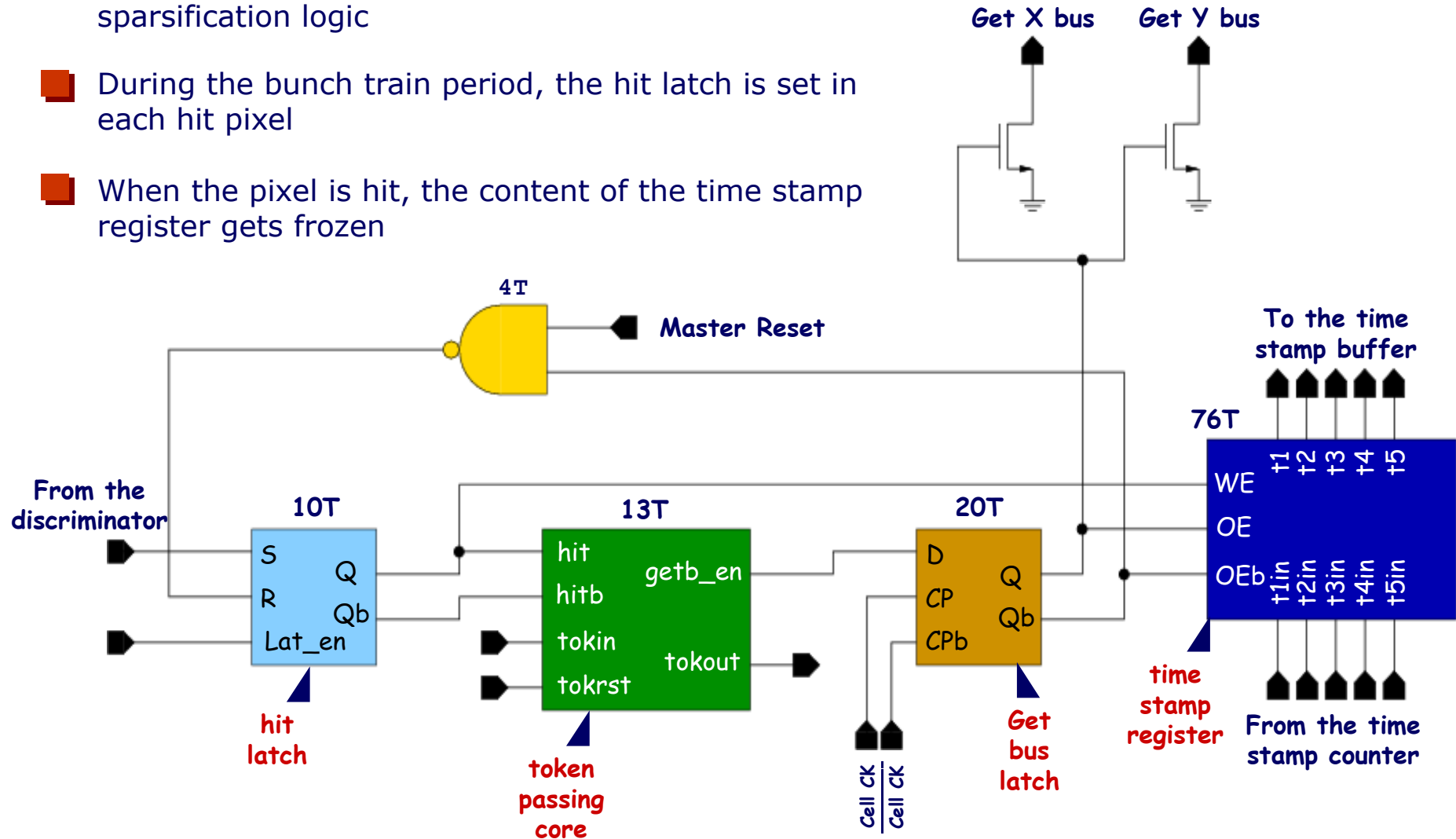


- $C_F$  obtained from the source-drain capacitance
- High frequency noise contribution has been reduced limiting the PA bandwidth
- ENC = **25  $e^-$  rms** @  $C_D = 100$  fF
- Threshold dispersion  $\approx$  **30  $e^-$  rms**
- Power consumption  $\approx$  **5  $\mu$ W**
- Features power-down capabilities for power saving: the analog section cell can be switched off during the intertrain interval in order to save power (**1% duty-cycle** seems feasible)



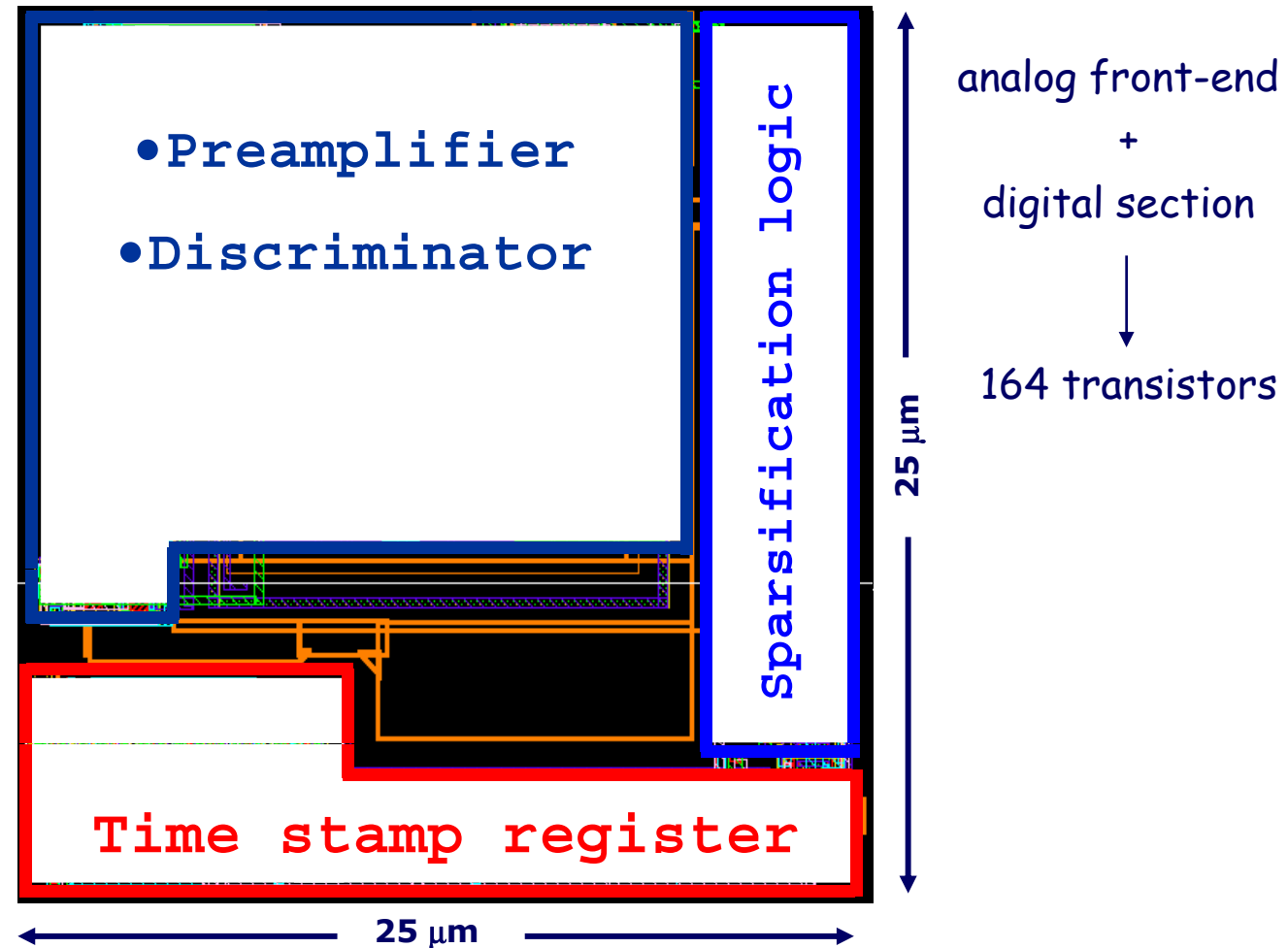
# Cell digital section

- Includes a 5 bit time stamp register and the data sparsification logic
- During the bunch train period, the hit latch is set in each hit pixel
- When the pixel is hit, the content of the time stamp register gets frozen

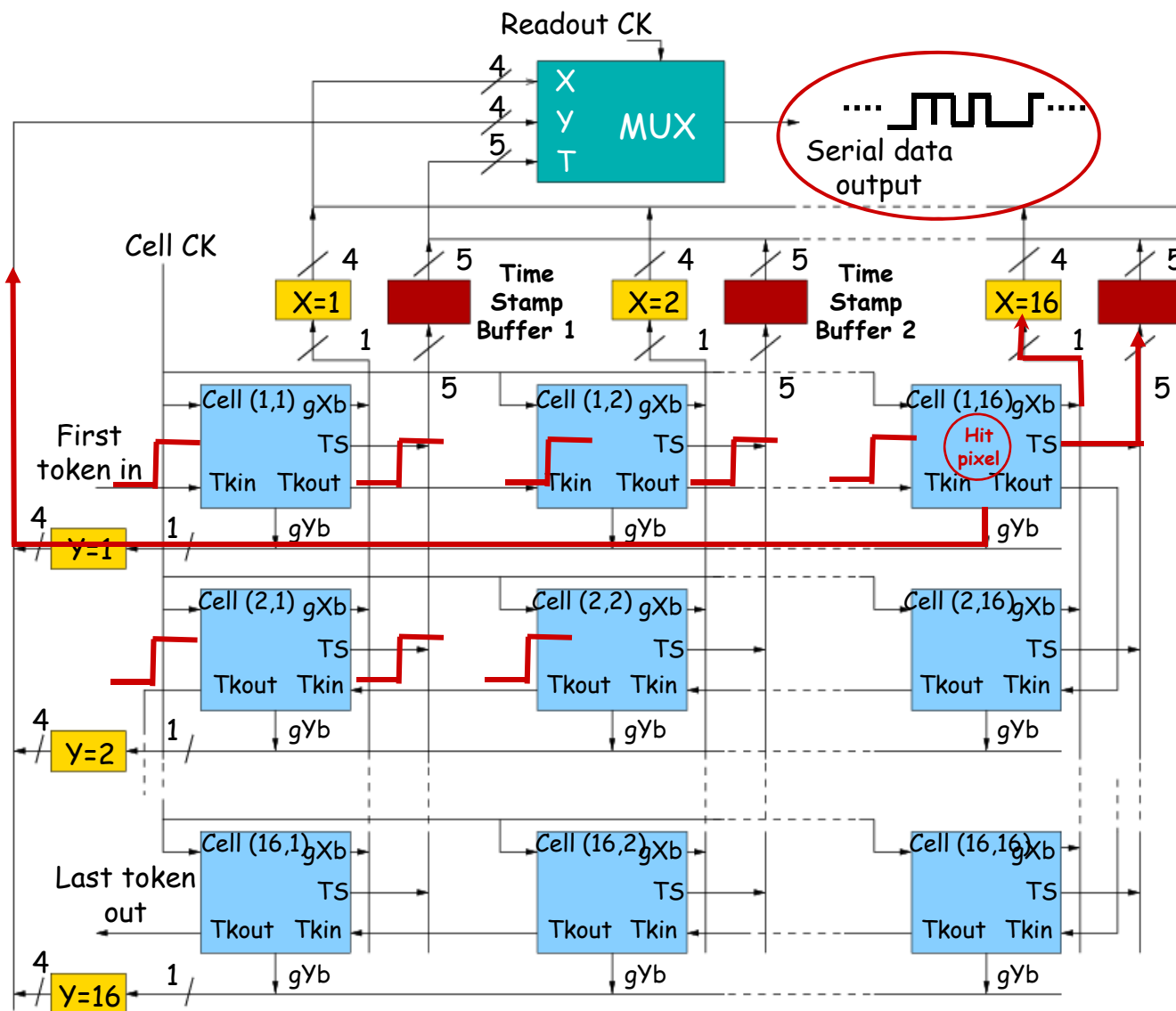


# ILC DNW elementary cell

10



# Digital readout scheme



Readout phase:

- token is sent
- token scans the matrix and
- gets caught by the first hit pixel
- the pixel points to the X and Y registers at the periphery and
- sends off the time stamp register content
- data are serialized and token scans ahead

The number of elements may be increased without changing the pixel logic (just larger X- and Y- registers and serializer will be required)

# Power dissipation analysis

- Because low material budget is necessary, there is little room for cooling system → very low power operation
- Analog power:  $P_{an,pix} \approx 5\mu\text{W}/\text{pixel}$  (dissipated in the analog PA)
- Digital power:  $P_{DC,pix} \approx 7\text{ nW}/\text{pixel}$  (leakage currents of the digital blocks)  
 (power in the periphery neglected since it grows as the square root of the number of matrix cells)  $P_{dyn,pix} \approx 20\text{ nW}/\text{pixel}$  (to charge the input capacitance of the time stamp register blocks during the detection phase)

$$P_{tot} = P_{an,pix} \cdot N \cdot M \cdot \delta_p + P_{DC,pix} \cdot N \cdot M + P_{dyn,pix} \cdot N \cdot M \cdot \delta_p$$

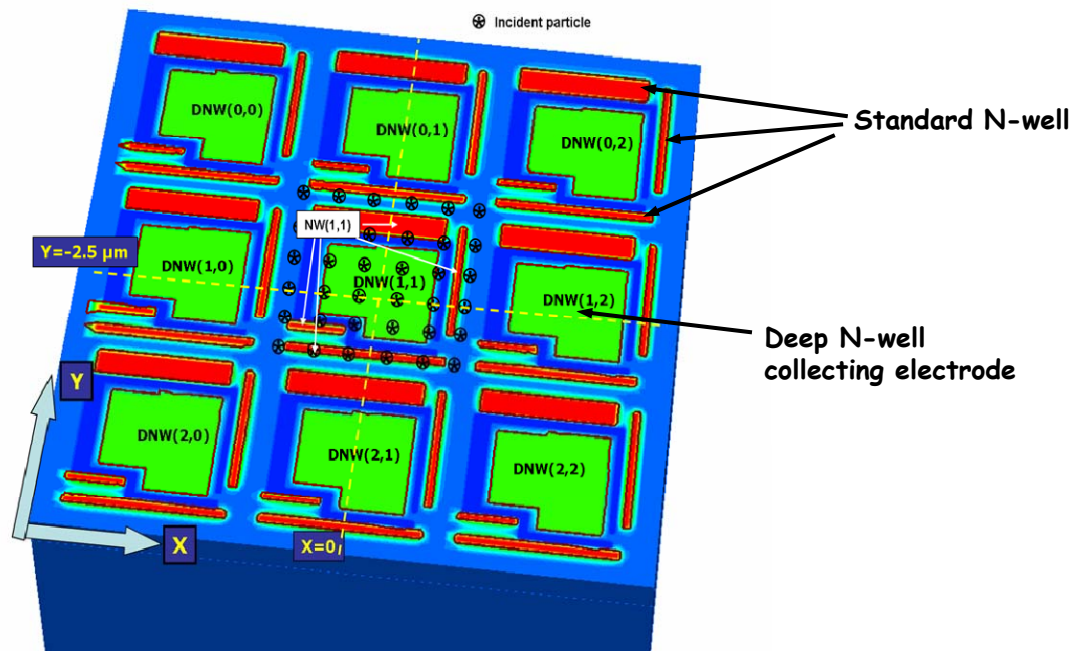
$\approx 15.5\text{ W}$        $13.6\text{ W}$        $1.9\text{ W}$        $0.05\text{ W}$

Assuming:

- 170000mm<sup>2</sup> total vertex detector area (pixel pitch of 25 μm);
- 1 Mpixel chips;
- $\delta_p=0.01$  power supply duty cycle

N= number of cell per pixel  
 M= number of chip composing the detector

# 3D device simulations



- The simulated structure (with TCAD) required a mesh with 165000 vertices. Because of the really long computation time only 36 simulations, each involving a different MIP collision point, have been performed

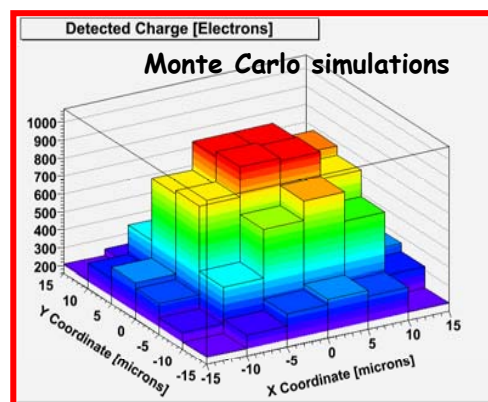
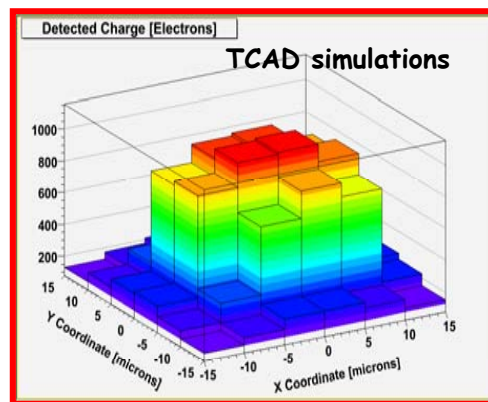
- MAPS operation is mainly diffusion driven → computing power required by TCAD may not be needed

- Monte Carlo code based on random walk developed (results of a collaboration with D. Christian - Fermilab)

- Activity presently focused on finely tuning a three-dimensional diffusion model for Monte Carlo simulations of MAPS by comparison with TCAD simulation results

- Advantage: dramatic reduction in computing time

- Next step: take advantage of fast Monte Carlo simulator to maximize detection efficiency through suitable layout choice



Charge collected by the central pixel in the  $3 \times 3$  SDR0 matrix  
Physical simulation performed by E. Pozzati - University of Pavia (Italy)

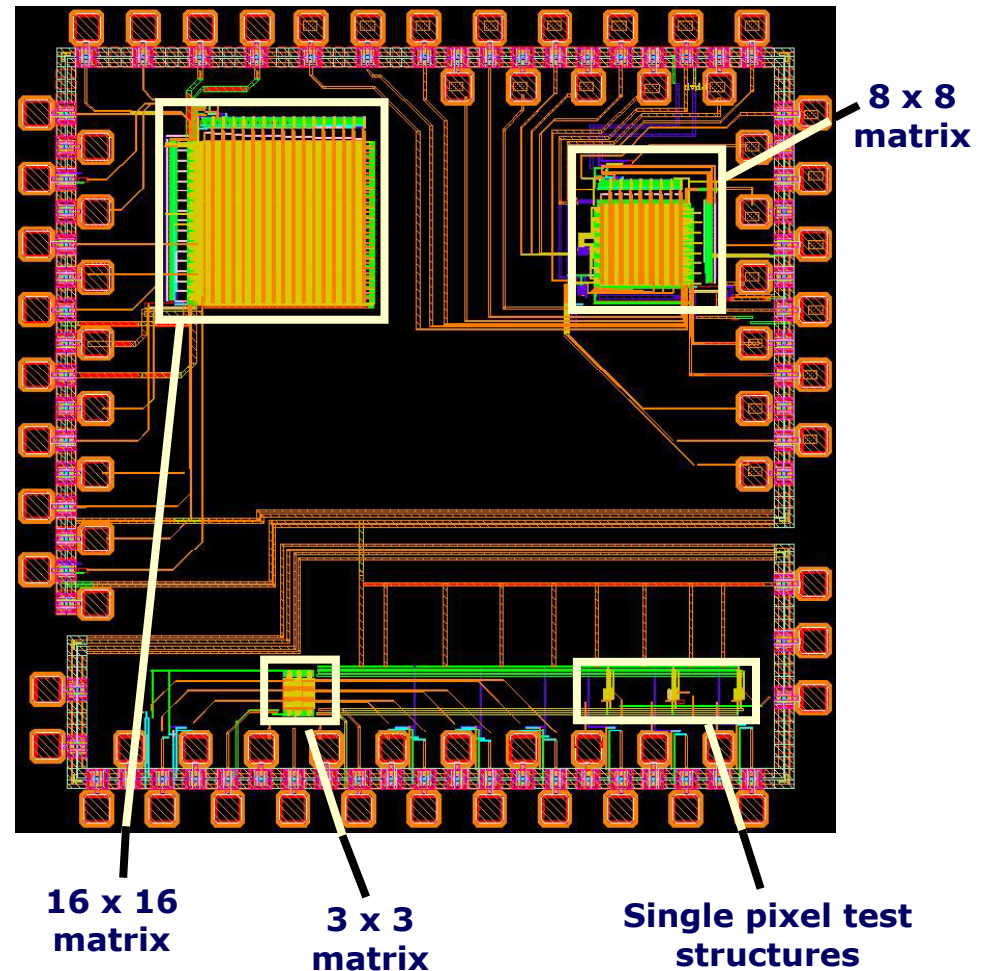
# The demonstrator chip (SDRO)

14

## ■ The chip includes:

- a 16 by 16 MAPS matrix (25  $\mu\text{m}$  pitch) with digital sparsified readout
- an 8 by 8 MAPS matrix (25  $\mu\text{m}$  pitch) with digital sparsified readout and selectable access to the output of the PA in each cell
- a 3 by 3 MAPS matrix (25  $\mu\text{m}$  pitch) with all of the PA output accessible at the same time
- 3 standalone readout channels with different  $C_D$  (detector simulating capacitance)

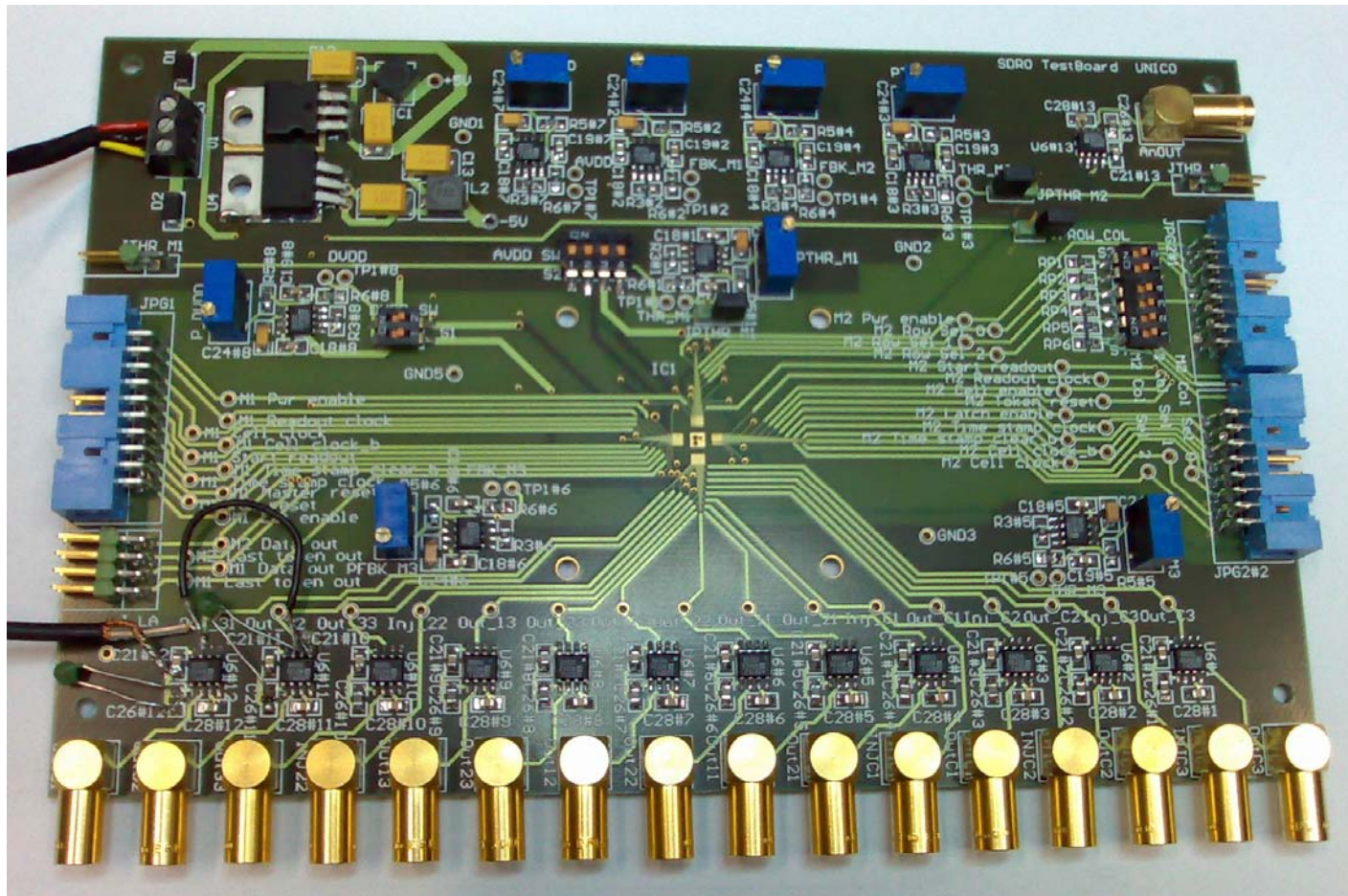
■ Delivered end of July 2007





# The SDR0 test board

15



Credit: Fabio Risigo University of Insubria, Como (Italy)

**Test board designed by Marcin Jastrzab**  
University of Science and Technology, Cracow  
(Poland) and University of Insubria, Como (Italy)

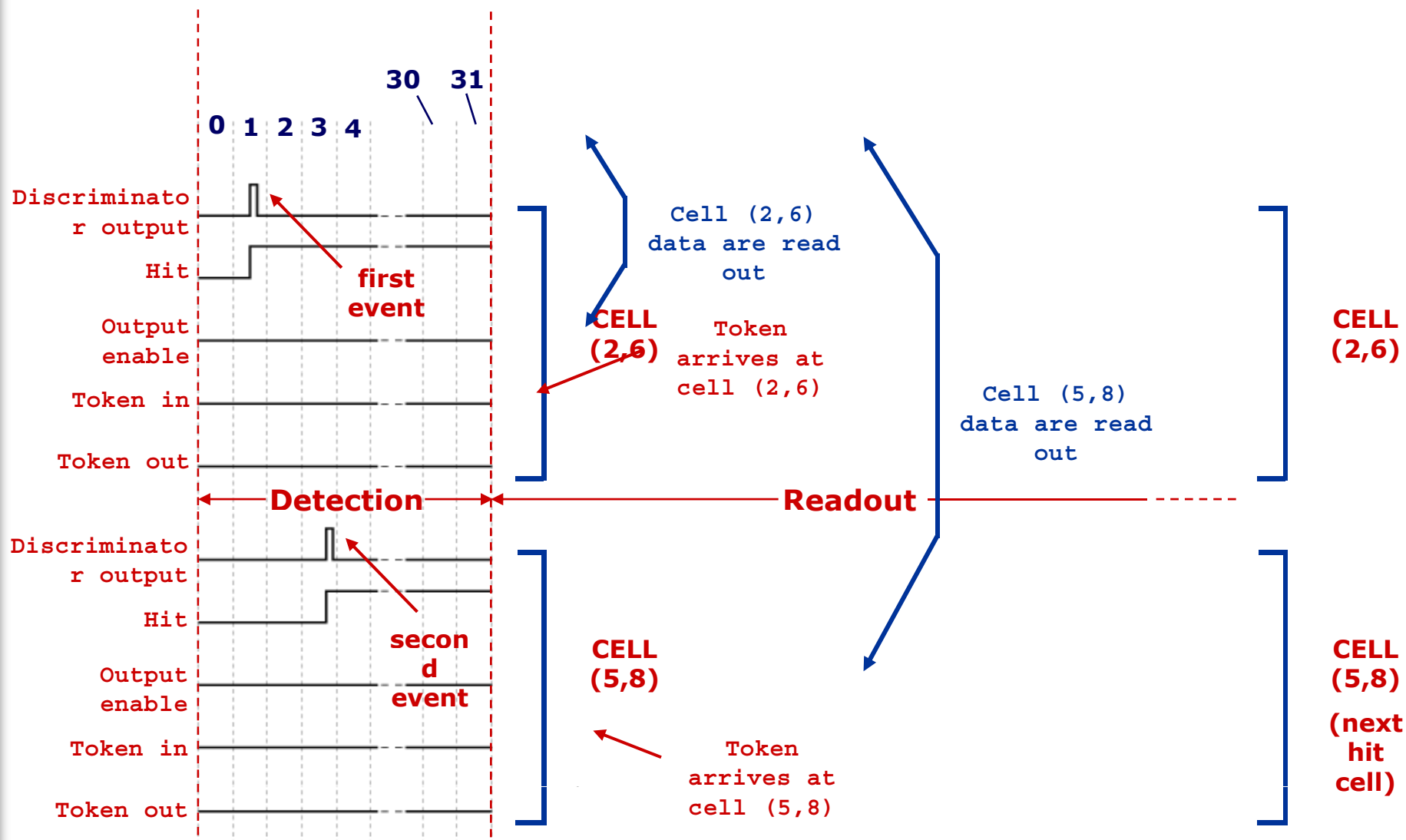
# Conclusions

- New DNW MAPS structures with optimized noise and threshold dispersion characteristics have been fabricated in the 130 nm, triple well STM CMOS technology
- Study of the charge collection efficiency and of charge spreading in the epi-layer is underway to assess their suitability for tracking and vertexing applications
  - Monte Carlo method will be used, besides Synopsys TCAD software package, in the design of the next generation prototype chips
- Characterization of a DNW MAPS demonstrator aimed at vertexing applications at the ILC is foregoing
- Plans for the future:
  - design of a 256 x 256 matrix for beam test
  - evaluation of more scaled technologies (90 nm CMOS)



# Backup slides

# Digital signal diagram



# Parameter mismatch

- Identically designed components always show discrepancies in the values of electrical parameters. Fluctuations are induced by microscopic variations in physical quantities (e.g. oxide thickness, doping concentration, device dimensions).
- In CMOS transistors threshold voltage  $V_{th}$  and channel transconductance  $g_m$  are typically affected; for instance, the threshold voltage variation  $\Delta V_{th}$  has a normal distribution with zero mean and a variance  $\sigma^2(\Delta V_{th})$  inversely proportional to the device gate area:

$$\sigma_{\Delta V_{th}}^2 = \frac{A_{vth}^2}{W \cdot L}$$

$A_{vt}$  is a constant provided by the foundry and included in the device parameter set

- As a design rule,  $\sigma_{\Delta V_{th}}$  can be reduced by acting on the device dimensions
- In the case of a charge processor with binary readout, parameter dispersion affects both the analog and the digital section

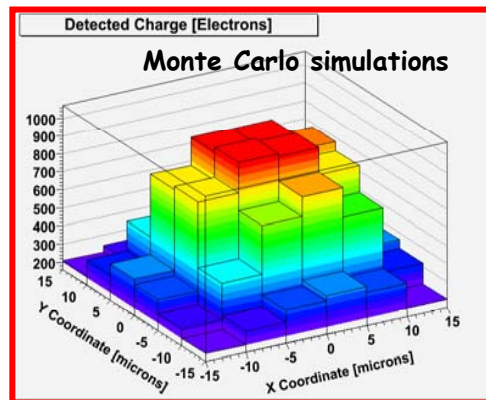
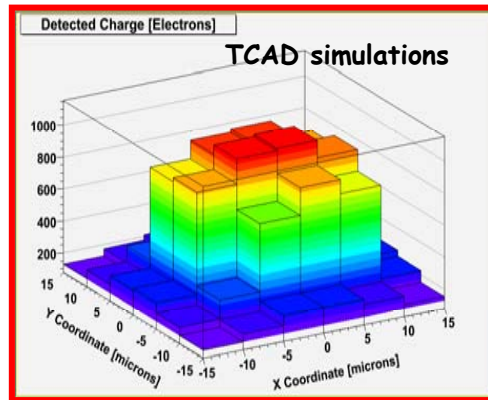
# Design specifications for the ILC vertex detector

SDR0 prototype

Hit rate [particles/bco/mm <sup>2</sup> ]	Detector pitch [ $\mu\text{m}$ ]					
	5	10	15	20	25	30
0.03	99.99%	99.97%	99.84%	99.52%	98.87%	97.76%
0.06	99.99%	99.87%	99.39%	98.20%	95.91%	92.26%
0.09	99.98%	99.72%	98.69%	96.20%	91.70%	84.93%
0.12	99.97%	99.52%	97.76%	93.68%	86.66%	76.75%
0.15	99.95%	99.26%	96.62%	90.75%	81.13%	68.36%

Detection efficiency for different sensor pitch and hit rate values

# 3D device simulations



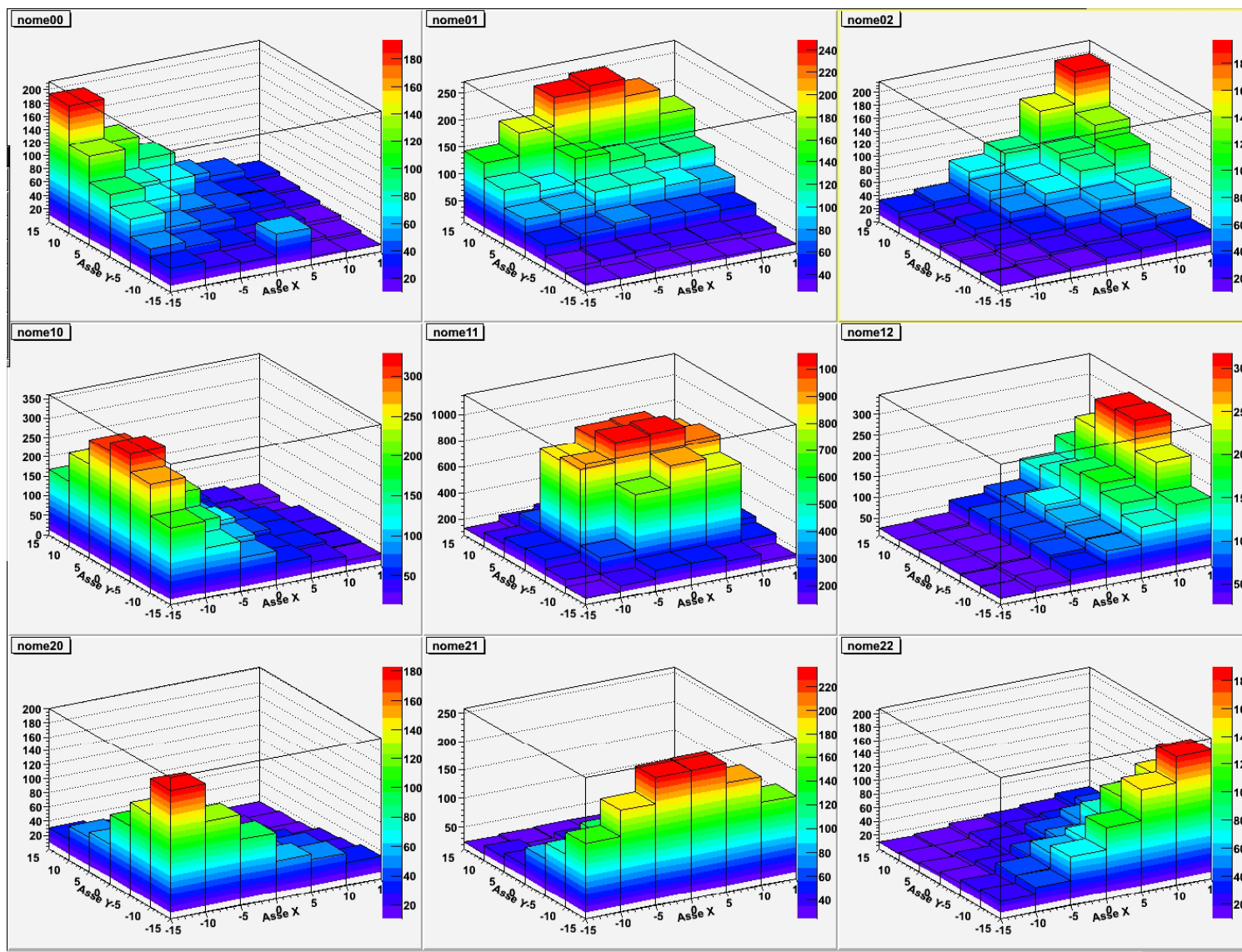
Charge collected by the central pixel in the  $3 \times 3$  SDR0 matrix  
Physical simulation performed by E. Pozzati - University of Pavia (Italy)

▪ E. Pozzati, M. Manghisoni, L. Ratti, V. Re, V. Speziali, G. Traversi:  
"MAPS in 130nm triple-well CMOS technology for HEP applications"  
Topical Workshop on Electronics for Particle Physics, TWEPP 2007,  
Sept. 3-5, Prague, Czech Republic

Simulations with Monte Carlo code have been performed with the following assumption:

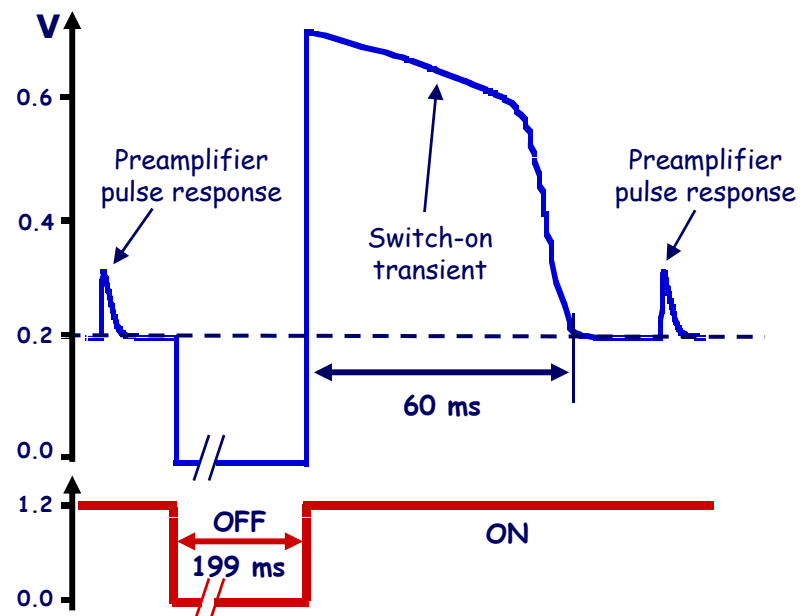
- 80 e-h/ $\mu\text{m}$  are generated uniformly along a linear track which is normal to the device surface and feature a gaussian distribution in the plane normal to the track itself ( $\sigma=0.5 \mu\text{m}$ ).
- The SDR0 simulation volume is  $85 \times 85 \times 80 \mu\text{m}^3$ .
- Electron lifetime, according to the Scharfetter model is about  $9.2 \mu\text{s}$  at the considered doping levels ( $10^{15} \text{cm}^{-3}$ ) and sets a limit to the random walk duration for each carrier.

# 3D device simulations



# Power cycling simulations

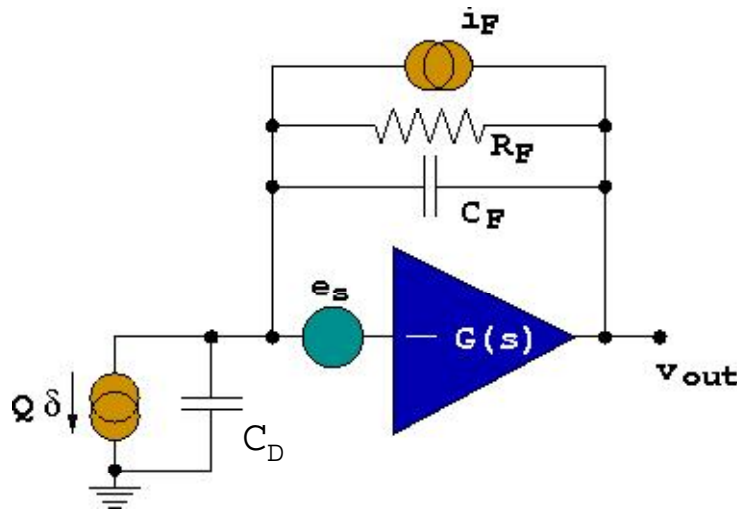
- Power cycling can be used to reduce average dissipated power by switching the chip off when no events are expected
- Example:
  - ✓ ILC bunch structure:  $\sim 330$  ns spacing,  $\sim 3000$  bunches, 5Hz pulse
- The analog section in the elementary cell can be switched off during the intertrain interval in order to save power (analog power is supposed to be predominant over digital)



- Based on circuit simulations, power cycling with at least **1% duty-cycle** seems feasible



# Noise performance analysis



For the forward stage of the charge preamplifier, a single pole transfer function can be reasonably assumed:

$$G(s) = \frac{G_0}{1 + \frac{s}{\omega_0}}$$

$$\left\{ \begin{array}{l} e_s = \sqrt{S_W + \frac{A_F}{f}} \leftarrow \text{Input referred series noise of the charge PA} \\ i_F = S_P \leftarrow \text{Parallel noise contribution in the feedback network} \end{array} \right.$$

Parallel noise contribution

$$ENC_{i_F} \approx \sqrt{S_P \cdot R_F \cdot C_F}$$

Series white noise contribution

$$ENC_{e_s, S_W} \approx \sqrt{S_W \cdot C_T \cdot C_F \frac{GBP}{2}}$$

$$C_T = C_D + C_{in} + C_F$$

$C_{in}$  is the charge PA input capacitance

Series 1/f noise contribution

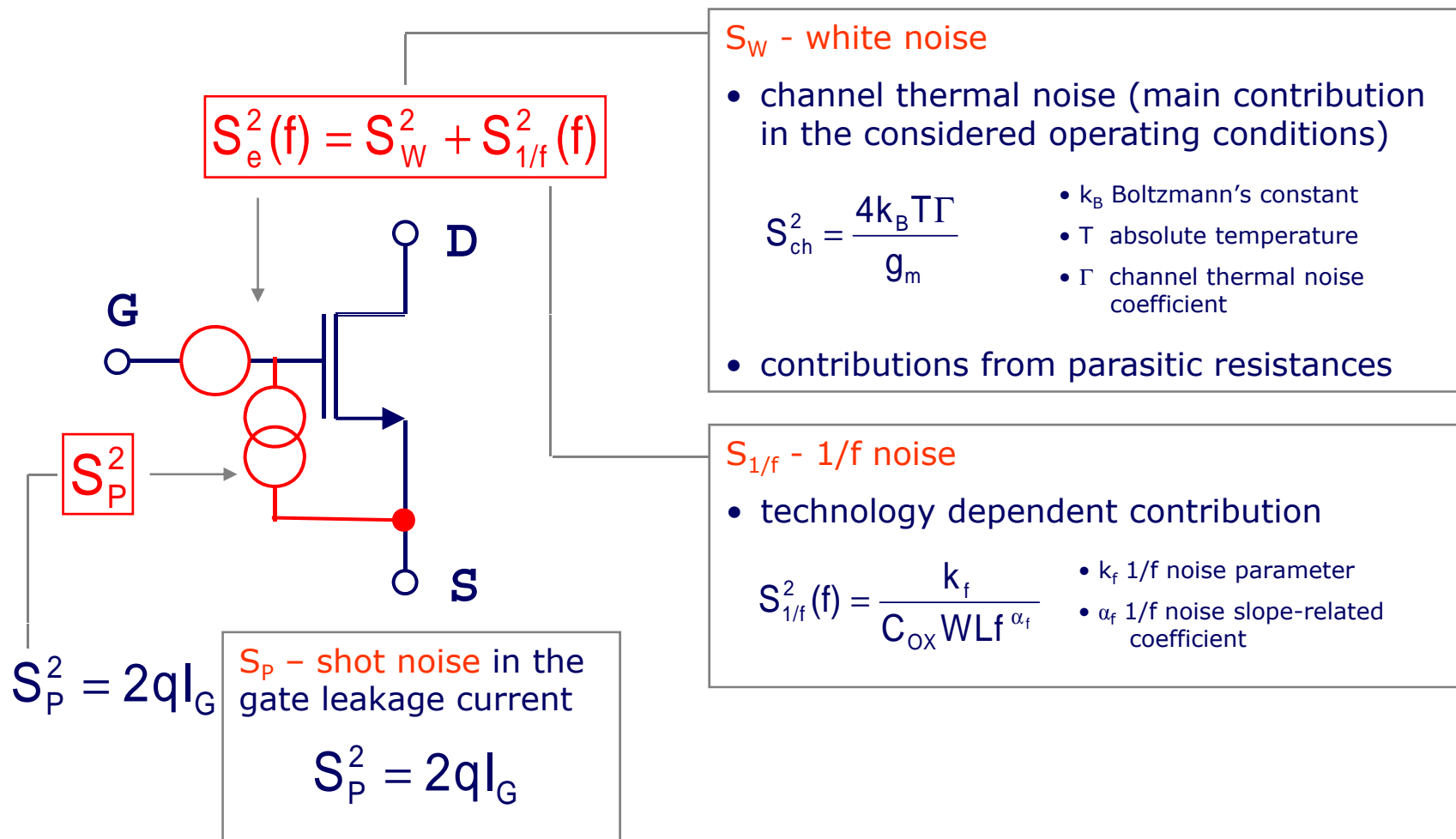
$$ENC_{e_s, 1/f} \rightarrow \infty$$

The mean square value of the noise due to 1/f contribution slowly diverges. Actually, divergence is so slow that this contribution is not supposed to affect significantly the noise properties of the analog front-end (in field operation times).

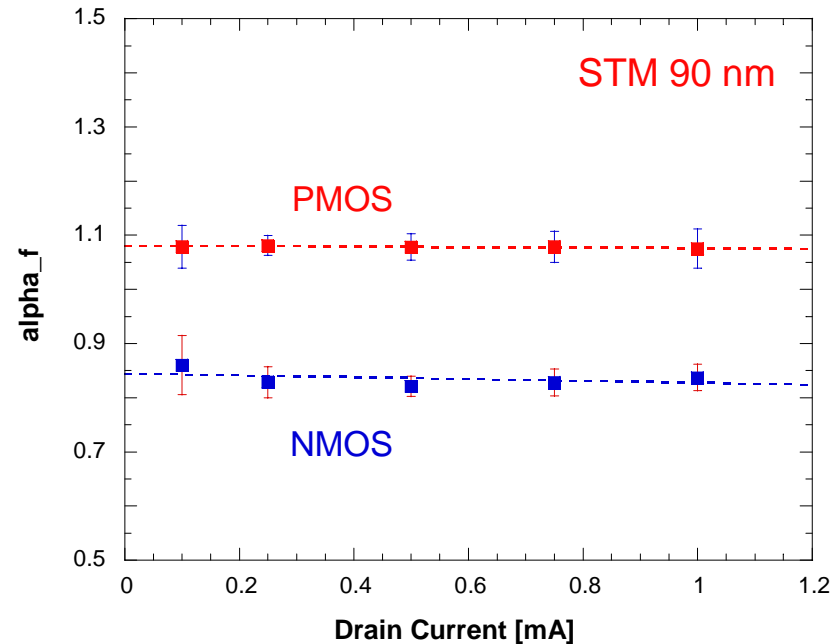
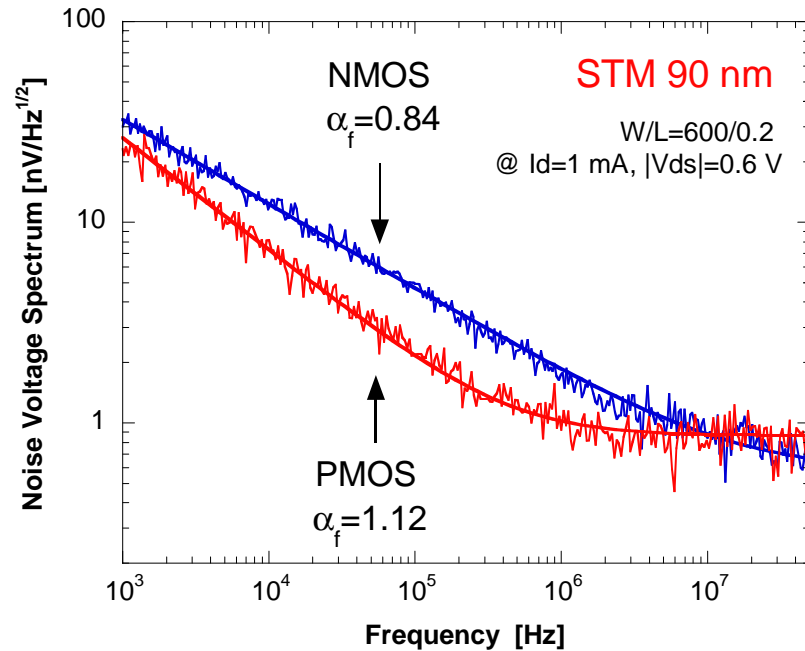


# Noise in CMOS transistors

- Noise in the drain current of a MOSFET can be represented through an equivalent noise voltage source in series with the device gate



# Flicker noise - $S_{1/f}(f)$



- Slope  $\alpha_f$  of the 1/f noise term is significantly smaller than 1 in NMOS transistors and larger than 1 in PMOS devices
- In the examined operating region,  $\alpha_f$  does not exhibit any clear dependence on the drain current or on the channel length
- $\alpha_f$  between 1 and 1.3 for PMOS devices, between 0.8 and 1 for NMOS devices

# The SLIM5 collaboration (Silicon Detectors with Low Interaction with Material - CSN5 INFN)

27

S. Bettarini<sup>1,2</sup>, A. Bardi<sup>1,2</sup>, G. Batignani<sup>1,2</sup>, F. Bosi<sup>1,2</sup>, G. Calderini<sup>1,2</sup>, R. Cenci<sup>1,2</sup>, *F. Forti*<sup>1,2</sup> (coordinator),  
M. Dell'Orso<sup>1,2</sup>, P. Giannetti<sup>1,2</sup>, M. A. Giorgi<sup>1,2</sup>, A. Lusiani<sup>2,3</sup>, G. Marchiori<sup>1,2</sup>, F. Morsani<sup>2</sup>, N. Neri<sup>2</sup>,  
E. Paoloni<sup>1,2</sup>, G. Rizzo<sup>1,2</sup>, J. Walsh<sup>2</sup>,

C. Andreoli<sup>4,5</sup>, E. Pozzati<sup>4,5</sup>, L. Ratti<sup>4,5</sup>, V. Speziali<sup>4,5</sup>, L. Gaioni<sup>4,5</sup>,

M. Manghisoni<sup>5,6</sup>, V. Re<sup>5,6</sup>, G. Traversi<sup>5,6</sup>,

L. Bosisio<sup>7</sup>, G. Giacomini<sup>7</sup>, L. Lanceri<sup>7</sup>, I. Rachevskaia<sup>7</sup>, L. Vitale<sup>7</sup>,

M. Bruschi<sup>8</sup>, A. Gabrielli<sup>8</sup>, B. Giacobbe<sup>8</sup>, N. Semprini<sup>8</sup>, R. Spighi<sup>8</sup>, M. Villa<sup>8</sup>, A. Zoccoli<sup>8</sup>,

D. Gamba<sup>9</sup>, G. Girauda<sup>9</sup>, P. Mereu<sup>9</sup>,

G.F. Dalla Betta<sup>10</sup>, G. Soncini<sup>10</sup>, G. Fontana<sup>10</sup>, L. Pancheri<sup>10</sup>, G. Verzellesi<sup>10</sup>

<sup>1</sup>Università degli Studi di Pisa, <sup>2</sup>INFN Pisa,

<sup>3</sup>Scuola Normale Superiore di Pisa,

<sup>4</sup>Università degli Studi di Pavia, <sup>5</sup>INFN Pavia,

<sup>6</sup>Università degli Studi di Bergamo,

<sup>7</sup>INFN Trieste and Università degli Studi di Trieste

<sup>8</sup>INFN Bologna and Università degli Studi di Bologna

<sup>9</sup>INFN Torino and Università degli Studi di Torino

<sup>10</sup>Università degli Studi di Trento and INFN Padova

## 4 Workpackages:

- 1 MAPS and Front End Electronics
- 2 Detectors on high-resistivity Silicon
- 3 Trigger / DAQ
- 4 Mechanics/Integration/Test-Beam